Catal Lett (2012) 142:930–935
DOI 10.1007/s10562-012-0861-x

ORIGINAL ARTICLES

Inverse Hysteresis Phenomena During CO and C_3H_6 Oxidation over a Pt/Al_2O_3 Catalyst

Ali Abedi · Robert Hayes · Martin Votsmeier · William S. Epling

Received: 2 May 2012 / Accepted: 19 June 2012 / Published online: 3 July 2012

Abstract It is well known that conversion as a function of temperature hysteresis can occur during ignition and extinction exothermic reaction experiments, such as CO oxidation over Pt/Al_2O_3, with the activity during the ignition process not matching that during the extinction process. Conversions being higher during extinction than that during ignition are often observed. Several explanations have been proposed in which heat effects, different catalyst surface states, and different Pt oxidation states are the most common. In this work CO oxidation hysteresis behavior, when in a mixture with C_3H_6, was investigated. The results show that when C_3H_6 was absent, CO oxidation followed normal hysteresis behavior; however, when C_3H_6 was added to the mixture, the catalytic activity during the extinction phase decreased. As the C_3H_6 concentration in the mixture increased, the hysteresis loop became smaller and ultimately reverse hysteresis was observed. The decrease in catalytic activity during extinction was due to the formation of C_3H_6 oxidation intermediate species. These species competed with CO for active sites, thus inhibiting CO oxidation, and were not present during ignition as CO was the dominant adsorbed species when starting at low temperature.

A. Abedi · W. S. Epling (✉)
Department of Chemical Engineering, University of Waterloo, Waterloo, ON, Canada
e-mail: wsepling@central.uh.edu

R. Hayes
Department of Chemical and Materials Engineering, University of Alberta, Edmonton, AB, Canada

M. Votsmeier
Automotive Catalysis Division, Research and Development, Umicore, Hanau, Germany

Keywords Diesel oxidation catalyst · CO oxidation · Propylene oxidation · Hysteresis

1 Introduction

Carbon monoxide (CO) and hydrocarbons (HCs) are pollutants emitted from vehicle engines. For diesel engines, diesel oxidation catalysts (DOCs) are used in aftertreatment systems to convert CO and HC species to CO_2 and H_2O. Even though DOCs provide very effective control of CO and HC emissions at higher temperatures, during cold start period significant amounts of CO and HCs pass unconverted through the catalyst [1, 2]. During the cold start period the catalyst temperature is too low for the reactions to take place. The oxidation of CO on Pt has been investigated in numerous studies, including in the classic work of Langmuir [3–9]. CO oxidation is known to occur through a Langmuir–Hinshelwood dual-site mechanism, in which the reaction occurs between CO and O_2 after both molecules adsorb on the surface [5, 10, 11]. Langmuir and co-workers observed that at high temperature and excess oxygen, active sites are entirely covered with oxygen and the reaction is limited by the rate at which CO adsorbs to the surface [3, 4, 8]. However, at low temperature the surface is covered with CO and the reaction is inhibited by strong adsorption of CO on the surface, a phenomenon known as CO self-poisoning [3, 6–8]. The effect of CO self-poisoning increases with increasing CO concentration [5] and decreases with increasing temperature, with negligible inhibition above 370 °C [4, 7]. Voltz et al. [7] found that at low temperature, CO and C_3H_6 are both self-inhibiting. Furthermore, in a $CO + C_3H_6$ mixture, CO inhibits C_3H_6 oxidation and vice versa due to competitive adsorption over catalytically active sites [7].

CO oxidation ignition and extinction studies show hysteresis behavior, with higher conversion during extinction [10–25]. Carlsson and Skoglundh [13] explained normal hysteresis as a combination of three possible reasons: (1) inherent kinetic bistability, (2) interaction between reaction kinetics and diffusion phenomena, and (3) locally high temperatures on the catalyst surface. Hysteresis, or multiplicity, in CO oxidation on Pt was discussed by Beusch et al. [12] who argued that the multiplicity exists when the intrinsic rates of the reaction and chemisorption steps are of equal size. An alternative explanation of hysteresis [17, 19, 20, 25] is the interaction between surface reaction and diffusion. Hegedus et al. [17] concluded that CO oxidation hysteresis behavior is due to the interaction of the negative-order kinetics for CO oxidation with the diffusive resistances of the catalysts. For example, the region of hysteresis was broadened by increasing the diffusion resistance of the tested Pt/Al_2O_3 catalyst by partially aging the catalyst [17]. Oh et al. [18], who investigated the role of intrapellet diffusion resistance in hysteresis during CO oxidation over $Pt\text{-}Al_2O_3$, also showed that the width of conversion-temperature hysteresis loop is a function of particle size and it could be eliminated if the catalyst particle size is very small. However, Carlsson et al. [10] concluded that CO oxidation hysteresis is associated with different rates by which Pt is oxidized and reduced as function of gas-phase composition, which could also be related to the different oxidation and reduction rates associated with different particle sizes. Another explanation was put forward by Gudkov et al. [15], who explained hysteresis by local "overheating" of the active sites on the catalyst, caused by relatively slow dissipation of the energy through dispersed catalyst particles. This was supported in other studies by Subbotin et al. [21–23]. According to their results, in an exothermic reaction, such as CO oxidation, the rate of heat liberated is larger than the rate of heat dissipated in the environment due to the support's (or inactive catalytic mass) low thermal conductivity in which heat is released. Therefore, during the extinction phase, when the temperature of the inlet gas decreases, the temperature drop over the catalyst surface lags, staying warmer. In addition, it has been observed that the width of hysteresis loop increases with increasing CO concentration [21–23]. In terms of Pt state, Salomons et al. [11] modeled CO oxidation during ignition and extinction using a LH mechanism, with a dissociative chemisorption step for oxygen requiring two surface sites, whereby ignition and extinction processes corresponded to the two states of predominantly CO covered or O_2 covered.

Unlike CO oxidation, Hauptmann et al. [16] have shown that NO oxidation on a Pt catalyst under excess oxygen conditions exhibits "inverse hysteresis" as the catalytic activity during ignition exceeds the activity during extinction. The reason for this inverse hysteresis behavior during NO oxidation is that Pt is oxidized by NO_2, and the oxide is less catalytically active than metallic Pt. As the temperature drops during extinction, the Pt is more highly oxidized than it was during ignition, leading to poorer performance. In addition, in a $CO/NO/O_2$ mixture, CO oxidation hysteresis behavior switches from normal hysteresis to inverse hysteresis, which the authors attributed to reversible oxidation of Pt [16].

In this study, the hysteresis behavior of CO oxidation in a $CO + C_3H_6$ mixture over a Pt/Al_2O_3 monolith catalyst was investigated. Specifically, it was observed that C_3H_6 had a negative effect on CO oxidation during extinction. To explain the impact, TPO experiments and in situ diffuse reflectance infrared Fourier transform spectroscopy (DRIFTS) were used, during ignition and extinction, to determine if this was due to temperature or surface changes as a function of the C_3H_6 exposure.

2 Experimental Methods

The $Pt/zeolite/Al_2O_3$ sample used, with a total Pt loading of 95 g/ft^3 based on total monolith volume, was provided in monolithic form by Umicore AG. The sample was 1″ in diameter with a length of 2.5″. The sample was inserted into a horizontal quartz tube, which was placed inside a Lindberg Minimite temperature controlled furnace. The temperature was measured with 2 K-type thermocouples located at radial centers of the catalyst; the front one placed 1 mm upstream of the catalyst and the back one just inside the outlet face of the catalyst. CO, C_3H_6, CO_2 and O_2 were supplied as compressed gas cylinders by Praxair, and N_2 was generated using a nitrogen generator manufactured by OnSite Gas Systems. The flow rates of the various gases were controlled by Bronkhorst mass flow controllers and water was introduced using a Bronkhorst CEM system. The effluent gas from the reactor was analyzed using a MKS MultiGas 2030 FTIR analyzer. A matrix of experiments with different CO and C_3H_6 concentrations was run, shown in Table 1, and in all experiments the feed also contained 10 % O_2, 10 % H_2O, 10 % CO_2, and a balance of N_2, at a space velocity of 25,000 h^{-1} at standard conditions. In all $CO + C_3H_6$ mixture experiments, the temperature was ramped from 90 to 160 °C at a rate of 3 °C/min. Then the ramping was stopped and the reactor was cooled by decreasing the temperature of the furnace back to 90 °C, with the ramp rate ~5 °C/min. Before each experiment the catalyst was treated with 10 % O_2 in N_2 for 20 min at 200 °C, then the catalyst was cooled down under N_2 to 90 °C for the next experiment.

Table 1 CO and C_3H_6 concentrations during TPO experiments

Run	CO (ppm)	C_3H_6 (ppm)
1	500	0
2	1000	0
3	1000	300
4	1000	500
5	1000	800

3 Results and Discussion

3.1 CO Oxidation

Figure 1 shows the results from temperature programmed CO oxidation of 500 and 1,000 ppm CO during the temperature ramp up (solid lines) and the temperature ramp down (dashed lines). The inlet gas temperatures corresponding to 50 % CO conversion, $T_{(50)}$, during ignition and extinction are listed in Table 2. These data show normal hysteresis behavior. Also, the temperature difference (ΔT) at 50 % conversion between the ignition and extinction increased with increasing CO concentration. Thus, the width of the hysteresis loop was larger with higher CO concentration. Such a trend has been previously observed in several studies [16–20, 22, 23] for the reasons explained in Sect. 1. A potential explanation, based on the possibilities listed in the Sect. 1, for the increase in activity during extinction is the catalyst surface or active sites being at a higher temperature than the measured temperature due to the heat generated by the exothermic reaction and thermal inertia of the catalyst (the catalyst temperature change lags behind the inlet temperature change during the ramp down) [16]. Data in Fig. 1 and temperature differences listed in Table 2 support this theory. It can also be related to Pt surface coverage and Pt chemical state [10, 13, 17], or a combination of these effects. As mentioned above, during ignition catalytic activity increases, but initially the Pt surface is predominantly covered with CO and the reaction is CO self-poisoned [10, 13, 26]. At higher temperature, once the reaction reaches complete conversion, all adsorbed CO is converted and the Pt surface becomes predominantly covered with O_2. Therefore, during extinction, as the temperature decreases below the temperature of complete conversion, the catalyst can remain active until adsorbed CO builds up, which is slowed due to the locally high temperatures of the active sites. The data in Fig. 1 indicate that CO coverage inhibited the reaction at low temperature, CO self-inhibition, and this affected the reaction during ignition of course, but only affects the extinction phase once the inlet gas temperature was much lower.

Table 2 Ignition and extinction $T_{(50)}$ CO oxidation values in a gas mixture including 10 % O_2, 10 % H_2O, 10 % CO_2, balanced by N_2 at a GHSV 25,000 h^{-1}

CO (ppm)	Ignition T (°C)	Extinction T (°C)	ΔT (°C)
500	95	87	8
1000	120	108	12

3.2 CO + C_3H_6 Oxidation

The results of TPO, during heating and cooling, with a CO and C_3H_6 mixture are shown in Figs. 2 and 3. The inlet gas mixture consisted of different C_3H_6 concentrations (300, 500, 800 ppm), 1,000 ppm CO, 10 % H_2O, 10 % O_2, 10 % CO_2, and balanced by N_2. Figure 2 shows CO conversion as a function of inlet gas temperature at different C_3H_6/CO

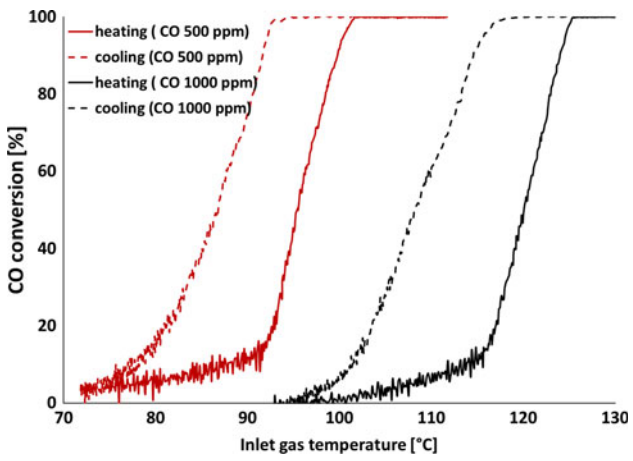

Fig. 1 Temperature-programmed CO oxidation with the following inlet conditions: 1,000 or 500 ppm CO, 10 % H_2O, 10 % CO_2, and 10 % O_2 over a Pt/Al_2O_3 monolith

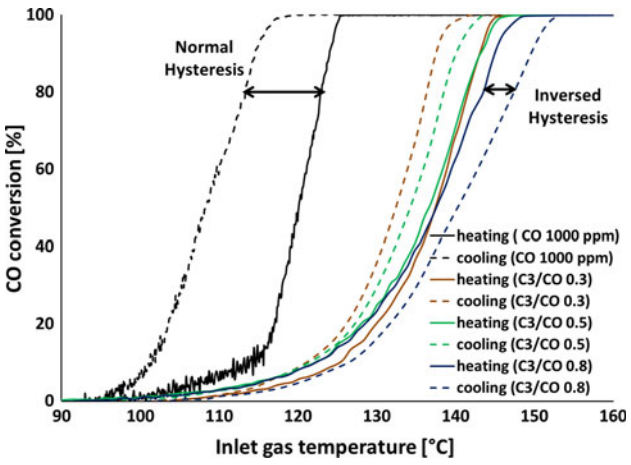

Fig. 2 Temperature-programmed oxidation of a CO/C_3H_6 mixture at the following inlet conditions: 1,000 ppm CO, 10 % H_2O, 10 % CO_2, 10 % O_2, with different amounts of C_3H_6 over a Pt/Al_2O_3 monolith

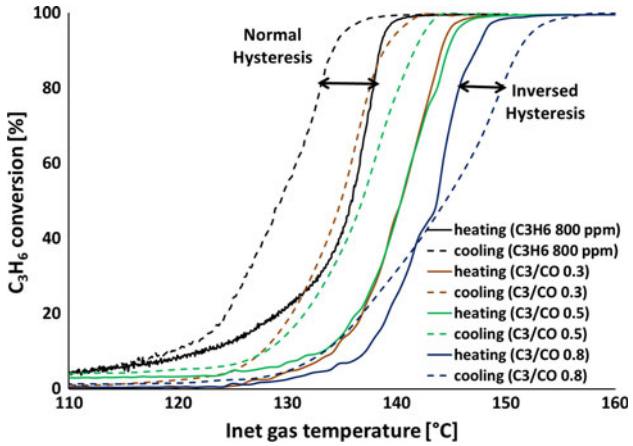

Fig. 3 Temperature-programmed oxidation of a CO/C_3H_6 mixture at the following inlet conditions: 1,000 ppm CO, 10 % H_2O, 10 % CO_2, 10 % O_2, and different amounts of C_3H_6 over a Pt/Al_2O_3 monolith

Table 3 ($T_{ignition} - T_{extinction}$) at $T_{(20)}$, $T_{(50)}$, and $T_{(80)}$, with different inlet C_3H_6 concentrations, 1,000 ppm CO, 10 % O_2, 10 % H_2O, 10 % CO_2, balanced N_2 at a GHSV 25,000 h^{-1}

CO (ppm)	C_3H_6 (ppm)	$\Delta T_{(20)}$ (°C)	$\Delta T_{(50)}$ (°C)	$\Delta T_{(80)}$ (°C)
1000	0	13	11	10
1000	300	2	5	5
1000	500	0	2	3
1000	800	−3	−3	−4

ratios. When C_3H_6 was not present in the inlet mixture, CO conversion exhibited normal hysteresis behavior as the ignition temperature at lower conversions was higher than those for extinction. However, when C_3H_6 was added to the mixture, the temperatures required to achieve certain conversions during the extinction phase increased and the hysteresis loop became smaller. Table 3 shows temperature differences between ignition and extinction corresponding to 20 %, 50 %, and 80 % conversion. As the C_3H_6/CO ratio increased, the extinction conversions continued to shift to higher temperature. At a 0.8 C_3H_6/CO ratio, the extinction temperatures, for conversions less than 100 %, became higher than the ignition temperatures, reverse hysteresis, as shown in Table 3 (with a negative difference between the ignition and extinction temperatures representing reverse hysteresis). C_3H_6 conversion as a function of inlet temperature is shown in Fig. 3. Like CO conversion, increasing the C_3H_6 concentration increased the temperatures to reach a certain conversion during the extinction phase and the hysteresis loop became smaller. Table 4 lists the temperature differences between the front and the back of the monolith at maximum conversion for the CO + C_3H_6 mixtures. The difference between front and back temperature, ΔT, increased with increasing C_3H_6 in the mixture, however, the hysteresis loop became

Table 4 Difference between back and front temperatures, ΔT, at maximum conversion with different combinations of CO and C_3H_6 with 10 % O_2, 10 % H_2O, 10 % CO_2, and balanced N_2 at a GHSV 25,000 h^{-1}

CO (ppm)	C_3H_6 (ppm)	ΔT (°C)
1000	0	23
1000	300	30
1000	500	38
1000	800	56

smaller as the temperature required to sustain maximum conversion increased during extinction. This is therefore not explained by the exothermic heat or overheating theory that was proposed in many studies, failing to explain the shift during the extinction phase to higher temperature instead of lower. Based on the overheating theory, the higher the concentration of reactant in the feed, the higher the exothermic heat released, and the larger the hysteresis loop should have become. However, these results with the CO/C_3H_6 mixture showed that the hysteresis loop became smaller when the C_3H_6 concentration, and consequently exothermic heat generated, increased.

3.3 DRIFT Spectroscopy

In situ DRIFTS was used to investigate species formation on the catalyst surface in the presence of the CO/C_3H_6 mixture during ignition and extinction tests. DRIFTS spectra were recorded at 100, 120, 140, and 160 °C, first increasing from 100 to 160 °C, as in ignition, then decreasing back to 100 °C, as in extinction. In order to understand the difference between what occurred during ignition versus extinction, in terms of catalyst surface coverage, DRIFTS spectra obtained with exposure of the Pt/Al_2O_3 powder to 1,000 ppm CO and 0 or 600 ppm C_3H_6 are shown in Fig. 4. In the absence of C_3H_6, the species formed on the surface, CO_2 at 2,300–2,400 cm^{-1}, blue circle, CO at 2,000–2,200 cm^{-1}, red circle, and carboxylate groups at 1,500–1,700 cm^{-1} [27–30], green circle, during ignition are similar to the those present during extinction, with the spectra overlapping, Fig. 4a, except for the peak at 1,596 cm^{-1} which corresponds to the presence of bidentate carbonate species on the surface during extinction. This peak indicates that bidentate carbonate species could be CO oxidation intermediates that built up on the surface as the temperature decreased during the extinction phase.

On the other hand, in the case of exposure to the CO + C_3H_6 mixture, Fig. 4b, more species are present during extinction than during ignition. The peaks between 2,300 and 2,400 cm^{-1} are assigned to CO_2 bound to Pt and

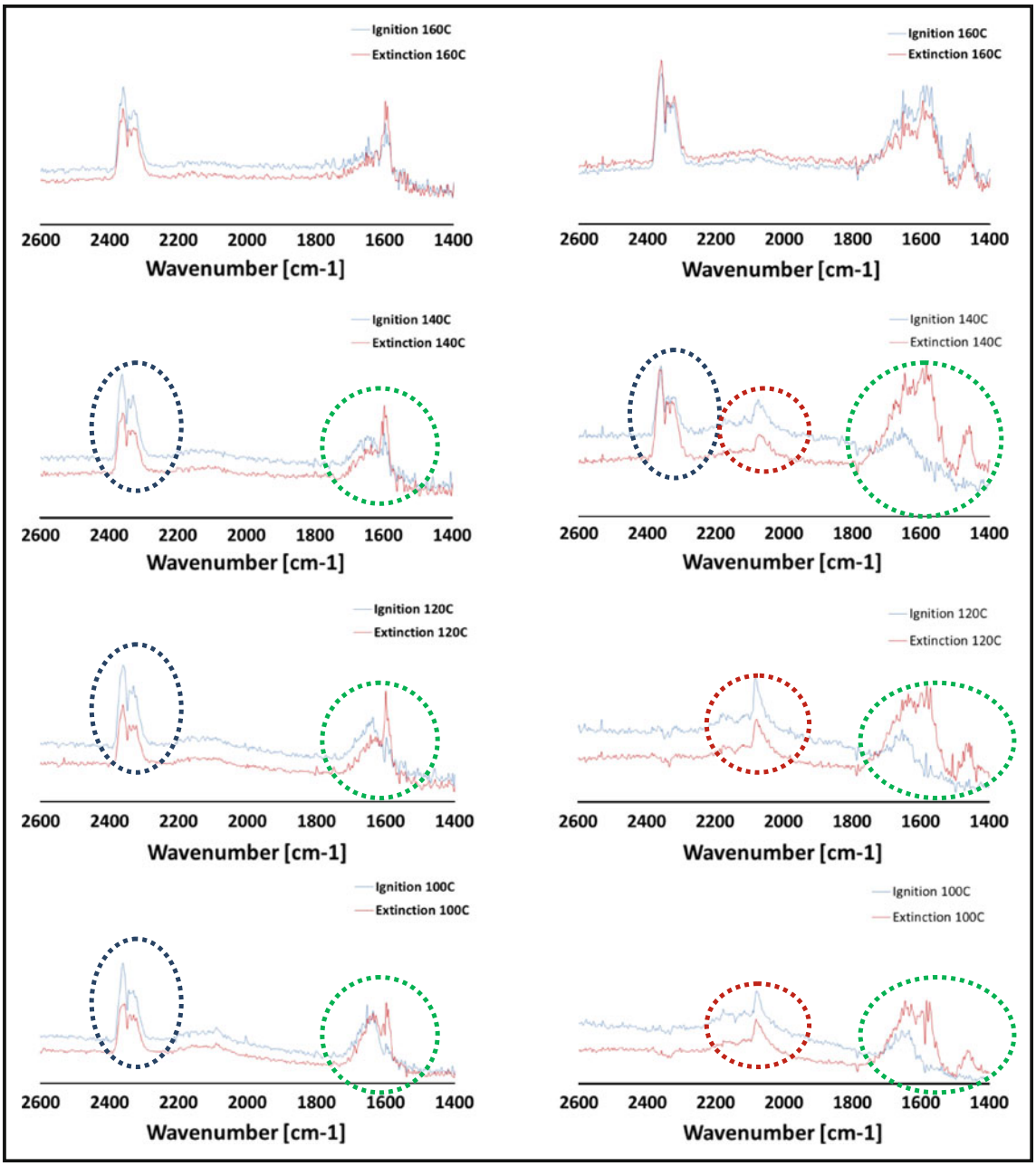

Fig. 4 DRIFTS spectra recorded during ignition and extinction phases at different steady state temperatures with 1,000 ppm CO and **a** 0 ppm C_3H_6 and **b** 600 ppm C_3H_6

CO_2 gas, and were present in both ignition and extinction and they follow the same trend in terms of intensity. Similarly, in both phases, the peak at 2,067 cm^{-1}, assigned to Pt bound CO, was seen at low temperature, but it disappeared at temperatures above 140 °C. Unlike Fig. 4a, at temperatures below 120 °C, the peak at 2,067 cm^{-1} (Pt–CO) was present and the peaks at 2,300–2,400 cm^{-1} (CO_2) were absent in Fig. 4b. The absence of the CO_2 peak, and the CO peak being present at higher temperatures, albeit this may be associated with C_3H_6 oxidation as discussed below, is consistent with C_3H_6 inhibition of CO oxidation [7]. Furthermore, CO is an intermediate product of C_3H_6 oxidation during the extinction process, as discussed below; therefore, in the presence of C_3H_6 the peak at 2,067 cm^{-1} appeared at higher temperatures and with greater intensity than in the absence of C_3H_6. The peaks increased in intensity as the C_3H_6 concentration increased. As verification, in tests with only C_3H_6 (i.e. with no CO in the mixture, data not shown), peaks in this range also appeared during extinction, demonstrating that these were

associated with C_3H_6 oxidation intermediates. For this reason, the CO peak in Fig. 4b is related to C_3H_6 oxidation rather than CO in the feed. In addition, between 1,700 and 1,300 cm^{-1} more peaks were observed in the presence of C_3H_6 in the mixture than in its absence, as shown in green circles in Fig. 4. For example, in the presence of C_3H_6 the peaks at 1662–1560, 1456, and 1388 cm^{-1}, associated with different carboxylic groups [27, 28, 30–33], were higher in intensity during extinction, relative to ignition. During extinction, as the temperature decreased, the oxidation of these intermediate species slowed, allowing them to remain longer and therefore build up. The peaks at 1,652 and 1,456 cm^{-1} are assigned to surface and bulk bicarbonates [27–30], respectively. The peaks at 1,585 and 1,388 are attributed to formate species [27, 31]. This indicates that in the presence of C_3H_6, more bicarbonate and formate species are present during the extinction process also. At high temperatures these intermediates were easily oxidized, but as the temperature dropped, they built up on the surface and compete with CO for active sites, thus inhibiting CO oxidation during the extinction process.

Overall, these results show that intermediate species form during C_3H_6 oxidation and that the amounts on the surface during ignition and extinction differ. The data suggest that during the extinction phase, these intermediates compete with CO for, or block CO from, active sites. For this reason, CO oxidation during the extinction phase was inhibited. The inhibition stems from the build up of different carboxylic, bicarbonate, and formate species as the temperature dropped. Thus, as the C_3H_6 concentration increased in the mixture, more intermediate species were present on the surface and CO oxidation conversions during extinction moved to higher temperature.

4 Conclusions

The oxidation of CO and CO + C_3H_6 over Pt/Al_2O_3 was studied, during both ignition and extinction. The results show that CO oxidation exhibits normal hysteresis in the absence of C_3H_6. However, in a CO + C_3H_6 mixture, as the C_3H_6 concentration increased in the mixture, CO and C_3H_6 normal hysteresis behavior shifted to inverse hysteresis, with the catalytic activity during the extinction phase lower than that during ignition. The decrease in catalytic activity during the extinction phase in the CO + C_3H_6 mixture was due to the formation of intermediate C_3H_6 oxidation species. These intermediate species, carboxylic groups, carbonates, and formates, compete with CO for active sites, thus inhibiting CO oxidation during extinction.

Acknowledgments The authors gratefully acknowledge AUTO21 for funding this work.

References

1. Tronci S, Baratti R, Gavriilidis A (1999) Chem Eng Commun 173:53
2. Twigg MV (2006) Catal Today 117:407
3. Engel T, Ertl G (1979) Adv Catal 28:1
4. Langmuir I (1922) Trans Faraday Soc 17:621
5. Salomons S, Votsmeier M, Hayes RE, Drochner A, Vogel H, Gieshof J (2006) Catal Today 117:491
6. Shishu RC, Kowalczyk LS (1974) Platin Met Rev 18:58
7. Voltz SE, Morgan CR, Liederman D, Jacob SM (1973) Ind Eng Chem Prod Res Dev 12:294
8. Wei J (1975) Adv Catal 24:57
9. Russell A, Epling WS (2011) Catal Rev Sci Eng 53:337
10. Carlsson P-A, Österlund L, Thormählen P, Palmqvist A, Fridell E, Jansson J, Skoglundh M (2004) J Catal 226:422
11. Salomons S, Hayes RE, Votsmeier M, Drochner A, Malmberg S, Gieshoff J (2007) Appl Catal B 70:305
12. Beusch H, Fieguth P, Wicke E (1972) Chem Ing Tech 44:445
13. Carlsson P-A, Skoglundh M (2011) Appl Catal B 101:669
14. Chakrabarty T, Silveston PL, Hudgins RR (1984) Can J Chem Eng 62:651
15. Gudkov BS, Subbotin AN, Yakerson VI (1999) React Kinet Catal Lett 68:125
16. Hauptmann W, Votsmeier M, Gieshoff J, Drochner A, Vogel H (2009) Appl Catal B 93:22
17. Hegedus LL, Oh SH, Baron K (1977) AIChE J 23:632
18. Oh SH, Baron K, Sloan EM, Hegedus LL (1979) J Catal 59:272
19. Schmitz RA (1975) Chem React Eng Rev 148:156
20. Smith TG, Zahradnik J, Carberry JJ (1975) Chem Eng Sci 30:763
21. Subbotin AN, Gudkov BS, Yakerson VI, Chertkova SV, Golosman EZ, Kozyreva GV (2001) Russ J Appl Chem 74:1506
22. Subbotin AN, Vorob'eva MP, Gudkov BS, Yakerson VI, Kustov LM (2002) Russ J Appl Chem 75:582
23. Subbotin AN, Gudkov BS, Dykh ZhL, Yakerson VL (1999) React Kinet Catal Lett 66:97
24. Usachev NY, Gorevaya IA, Belanova EP, Kazakov AV, Kharlamov VV (2004) Mendeleev Commun 14:79
25. Wei J, Becker R (1975) Adv Chem Ser 143:116
26. Carlsson PA, Skoglundh M, Fridell E, Jobson E, Andersson B (2002) Catal Today 73:307
27. Epling WS, Peden CHP, Szanyi JN (2008) J Phys Chem C 112:10952
28. Lercher JA, Colombier C, Noller H (1984) J Chem Soc 80:949
29. Morterra C, Ghiotti G, Boccuzi F, Coluccia S (1978) J Catal 51:299
30. Toops TJ, Smith DB, Epling WS, Parks JE, Partridge WP (2005) Appl Catal B 58:255
31. Iordan A, Zaki MI, Kappenstein C (1993) J Chem Soc 89:2527
32. Kantschewa M, Albano EV, Etrtl G, Knozinger H (1983) Appl Catal 8:71
33. Krupay BW, Amenomiya Y (1981) J Catal 67:362